ELSEVIER

Biochimica et Biophysica Acta 1460 (2000) 276–290

BIOCHIMICA ET BIOPHYSICA ACTA

BBA

www.elsevier.com/locate/bba

An elementary kinetic model of energy coupling in biological membranes

Ernesto Cristina, Julio A. Hernández *

Sección Biofísica, Facultad de Ciencias, Universidad de la República, Iguá s/n, esq. Mataojo, 11400 Montevideo, Uruguay

Received 19 August 1999; received in revised form 6 June 2000; accepted 8 June 2000

Abstract

The purpose of this work is to contribute to the understanding of the fundamental kinetic properties of the processes of energy coupling in biological membranes. For this, we consider a model of a microorganism that, in its plasma membrane, expresses two electrogenic enzymes (E_1 and E_2) transporting the same monovalent cation C and electrodiffusive paths for C and for a monovalent anion A. E_1 (E_2) couples transport C to the reaction $S_1 \leftrightarrow P_1$ ($S_2 \leftrightarrow P_2$). We developed a mathematical model that describes the rate of change of the electrical potential difference across the membrane, of the internal concentrations of C and A, and of the concentrations of S_2 and P_2. The enzymes are incorporated via two-state kinetic models; the passive ionic fluxes are represented by classical formulations of electrodiffusion. The microorganism volume is maintained constant by accessory regulatory devices. The model is utilized for stationary and dynamic studies for the case of bacteria employing the electrochemical gradient of Na^+ as energetic intermediate. Among other conclusions, the results show that the membrane potential represents the relevant kinetic intermediate for the overall coupling between the energy donor reaction $S_1 \leftrightarrow P_1$ and the synthesis of S_2.

Keywords: Membrane; Energy coupling; Ion pump; Mathematical model

1. Introduction

Many characteristic properties of cells are a consequence of the integrated functioning of membrane transport processes. As classical examples, the cell volume, the electrical potential difference across the cell membrane and the intracellular ionic composition of animal cells are the result of the integration of several passive and active processes of ionic transport occurring at the plasma membrane [1–3]. The processes of energy coupling that take place in the membranes of organelles and microorganisms represent further examples of relevant cellular phenomena depending on the simultaneous activity of diverse membrane transport systems [4,5]. These free energy transducing devices are supramolecular membrane complexes consisting of transport enzymes and of other intermediate receptors [6]. Most of the transport enzymes participating in the processes of energy coupling in membranes are electrogenic [7]: they couple a chemical source of free energy (e.g., a redox reaction) to the net charge movement resulting from the transmembrane transport of an ionic species (e.g., H^+ or Na^+). According to the chemiosmotic hypothesis, the electrochemical gradient generated by ionic pumping by some of these electrogenic enzymes (e.g., the cytochrome oxidase) is employed as a source of free energy by others (e.g., the F_0F_1-ATPase) for the uphill synthesis of ATP. The un-

* Corresponding author. Fax: +598-2-525-8629; E-mail: jahern@fcien.edu.uy

0005-2728/00/$ – see front matter
PII: S0005-2728(00)00153-5

coupled dissipation of the electrochemical gradients (ion leaks) represents an accessory component of the processes of cellular respiration; its molecular nature and physiological role are matters of discussion and active investigation [8,9].

The theoretical analysis of integrated models of membrane transport has provided an invaluable tool for the interpretation and prediction of experimental behavior in diverse cellular processes. This type of studies have constituted a classical topic in the biophysics of the plasma membrane of eukaryotic cells. Thus, diverse authors have proposed explicit physicochemical formulations to describe steady-state [10–17] and dynamic [1,18–21] properties of magnitudes dependent on transport processes across the plasma membrane (e.g., the membrane potential, the cell volume and some intracellular ionic concentrations, see above). For the case of energy coupling phenomena in membranes, the theoretical studies of the overall processes have mostly employed formalisms from irreversible thermodynamics or from metabolic control theory [4,5,22], approaches generally restricted to the linear domain near equilibrium or stationary states. Some authors have developed dynamic models using the kinetic approach [23,24], thus extending the analysis to the nonlinear region. In most cases, the nonlinear character of these models confines the studies to numerical simulations of stationary and time-dependent situations. In these latter models, the passive and active ion fluxes are generally represented by empirical expressions consistent with some kinetic properties. An important contribution to the theoretical analysis of dynamic models of energy coupling in membranes would be to incorporate the enzymatic ion transports in the form of explicit kinetic diagrams, in particular, those including electrogenic properties [7,25]. This would, for instance, permit to perform a more accurate evaluation of the kinetic role of the diverse participants in the process of energy coupling, like the electrical potential difference across the supporting membrane.

The general purpose of this study is to contribute to the understanding of the basic stationary and dynamic properties of the processes of energy coupling in membranes. In particular, we are concerned about the kinetic role of the fundamental participants (e.g., the electrical potential difference across the membrane and the intracellular concentration of the transported ion). In order to maximally reduce the complexity of the system, we consider in this work the case of a process of energy coupling occurring at the plasma membrane of an ideal microorganism, mediated by the integrated functioning of two electrogenic enzymes. For this case, we develop and study here a dynamic model that describes the rate of change of the electrical potential difference across the membrane, of the internal concentrations of a monovalent cation (C) and a monovalent anion (A), and of the concentrations of an energetic metabolite (S_2) and its degradative product (P_2). The model does not consider any mechanism of feedback control. The two electrogenic enzymes, E_1 and E_2, couple the transport of C to the chemical reactions $S_1 \leftrightarrow P_1$ and $S_2 \leftrightarrow P_2$, respectively. Both C and A experience electrodiffusion. The electrogenic enzymes are represented via two-state kinetic models that explicitly incorporate the effect of the membrane potential difference [25]. Rather straightforward considerations permit to suggest that, of the two energetic components comprising the electrochemical gradient that mediates the chemiosmotic coupling, the electrical potential difference across the membrane provides with a faster and less saturable source of free energy than the concentration component [7]. One of the particular objectives of the work presented here is to test this notion within the more complex frame of an integrated model of energy coupling. The two electrogenic enzyme design considered here, although simple from a biological perspective, is nevertheless sufficiently complex for analytical purposes. The finding that this elementary design indeed operates in certain bacteria employing the electrochemical gradient of Na^+ as intermediate for the coupling process [26,27] justifies its study as the minimal model for the description of free energy transduction in supramolecular membrane systems. A preliminary version of this work was presented at the 27th Annual Meeting of the Sociedad Argentina de Biofísica, held at La Plata, Argentina, in December 1998.

2. Mathematical model

The microorganism model employed here to derive

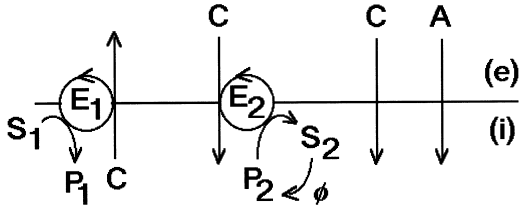

Fig. 1. Scheme representing the diverse fluxes taking place across the membrane of the microorganism, between the external (e) and internal (i) compartments. The scheme includes two electrogenic ion pumps (E_1 and E_2) transporting the same monovalent cation C, a diffusive path for C and a diffusive path for a monovalent anion A. E_1 (E_2) couples transport C to the chemical reaction $S_1 \leftrightarrow P_1$ ($S_2 \leftrightarrow P_2$). The path specified by ϕ represents the metabolic consumption of S_2.

the mathematical model has the following general characteristics (Fig. 1, see also Section 1):

1. The microorganism consists of a single homogeneous compartment, immersed in a large homogeneous medium of constant composition. We only consider here some transport events that could take place at the inner membrane.
2. The volume of the microorganism remains constant, due to the action of accessory volume regulatory devices that do not affect the variables considered here (e.g., volume regulation may occur via induced transport of electroneutral organic osmolytes [28–30]). As a consequence, the total area of the microorganism surface available for solute transport (A_c) also remains constant.
3. The plasma membrane contains separate diffusive paths for C and A (ion leaks), and the two ion pumps (E_1 and E_2) coupling the transport of C to chemical reactions. Although bacteria employing the electrochemical gradient of Na^+ as energetic intermediate do not seem to possess significant uncoupled diffusive pathways for this ion [26,31], we nevertheless included a cation leak (and, correspondingly, a complementary anion leak) in the model in order to evaluate its possible role in certain cases. In the Appendix we derive expressions for the steady-state fluxes of C mediated by the enzymes, from the analysis of explicit kinetic models (Fig. 2). The employment of these expressions in the overall dynamic model implicitly assumes that the enzymatic reactions achieve the steady-state condition several orders of magnitude faster than the internal solute concentrations. For simplicity, we considered the stoichiometric ratio between the enzyme-mediated flux of C and the coupled utilization of S_1 or S_2 to be the unity; this might not be the case in actual bacterial systems employing the electrochemical gradient of Na^+ as the energetic intermediate [26,32] (see below).

Under assumptions 1–3, the following mathematical model governs the rate of change of the internal concentrations of C, A, S_2 and P_2 (C_i, A_i, S_2 and P_2), and of the electrical potential difference across the plasma membrane (V_m, defined as $V_m = V_{outside} - V_{inside}$):

$$\begin{aligned} dC_i/dt &= (A_c/V_c)\,(-J_1 - J_2 + J_C) \\ dA_i/dt &= (A_c/V_c)\,(J_A) \\ dS_2/dt &= -dP_2/dt = (A_c/V_c)\,(-J_2 - \phi) \end{aligned} \tag{1a}$$

In order to obtain the time dependence of V_m, we employed a stationary solution of the electroneutral condition [16,21] (Appendix):

$$-J_1 - J_2 + J_C - J_A = 0 \tag{1b}$$

In Eqs. 1a and 1b, J_1 and J_2 are the fluxes of C mediated by the electrogenic enzymes (Eqs. A1 and A5); J_C and J_A are the corresponding electrodiffusive fluxes (Eq. A7), and ϕ is the rate of consumption of S_2 due to metabolic usage (Eq. A8; see the Appendix for assumptions and explicit expressions). From the

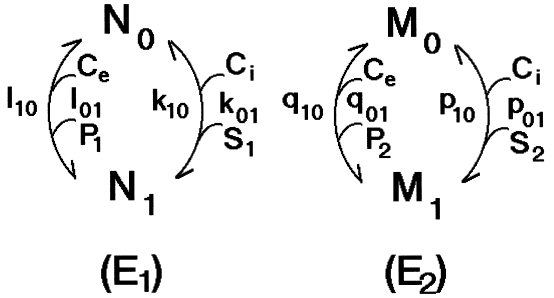

Fig. 2. State diagrams of the processes of transport of C mediated by the electrogenic enzymes E_1 and E_2. N_0, N_1 and M_0, M_1 are the corresponding intermediate states of the enzymes. C_i and C_e are internal and external C concentrations, respectively. The diagrams also include the other participating species (S_1, P_1 and S_2, P_2) and the true rate constants governing the corresponding transitions (k_{01}, k_{10}, l_{01}, l_{10} and p_{01}, p_{10}, q_{01}, q_{10}).

inspection of Eqs. 1a and 1b we can promptly notice that the steady-state requires equivalence in the magnitudes of the active and passive fluxes of C, electrochemical equilibrium of A, and exact balance between the production of S_2 by chemiosmotic coupling and its metabolic utilization. Eqs. 1a and 1b likewise assume that the consumption of S_2 via the metabolic flux ϕ also produces P_2. To be noted, the expressions employed here to represent ionic electrodiffusion (Eq. A7) satisfy Ohmic rectification [2], hence, they may not apply as such to the description of ionic leaks in some proton-mediated processes of energy coupling (e.g., as in mitochondria [33]).

Eq. 1a and 1b also imply the following conservation conditions:

$$S_2 + P_2 = T_2, \text{ and } C_i - A_i = q, \quad (2)$$

where T_2 and q are constants. The second equation is a consequence of the maintenance of macroscopic electroneutrality; we assumed that q is positive and counterbalanced by an equivalent amount of negative charges provided by non-diffusible ('fixed') intracellular anions. From the above, the three primary dependent variables to be considered are V_m, C_i and S_2.

In Section 3, we perform numerical studies of the model for the case of bacteria employing the electrochemical gradient of Na^+ as intermediate for the coupling process [26,31,34,35]. These studies are not exhaustive, and are only intended to illustrate some basic properties. Some particular issues considered here are: (a) the dependence of the steady-state on the model parameters; (b) the dynamic effect of the deprivation of S_1 and of the increment in S_1 ('S_1 pulse') on the model variables; (c) the dynamic effect of modifications in the rate of metabolic consumption of S_2, and (d) the dynamic effect of pulses of S_1, for the particular cases that V_m or C_i remained constant. In general, the dynamic effects produced by the perturbations are evaluated by the changes provoked on V_m, on C_i, and on the concentration of the energetic metabolite S_2. There is still little experimental evidence available from actual bacteria to compare with most of the theoretical results obtained here. For this reason, whenever applicable, we considered relatively large ranges of the numerical values of some of the parameters, in order to overspread possible physiological conditions.

3. Numerical results and discussion

3.1. Numerical methods

The methodology employed here is analogous to the one previously used by us to study a dynamic model of cell volume regulation in animal cells [21]. In order to perform the simulations, Eqs. 1a and 1b were integrated numerically employing the Runge–Kutta fourth order method, except for the determination of V_m. As mentioned above, after every time step, V_m was calculated assuming Eq. 1b by employing a stationary approximation including the electrogenic components (Appendix) [16,21]. For the particular conditions, the steady-state values of the variables were initially obtained from the corresponding time integrations and confirmed by an iterative procedure (Appendix). For the dynamic studies, we assumed that any modification of the metabolic requirement for S_2 took place abruptly, via instantaneous changes in the maximum rate ϕ_{max}. However, we introduced a more realistic time course of the induced modifications in the nutritional substrate S_1 by assuming

$$S_1(t) = S_1(\text{inf})\,[1-\exp(-t/\theta)] + S_1(0)\exp(-t/\theta), \quad (3)$$

where $S_1(0)$ and $S_1(\text{inf})$ are the initial (e.g., reference) and final (induced) values of S_1 respectively, and θ is the time constant.

3.2. Reference states

Unless specified, the numerical values of the parameters employed for the simulations were the ones shown in Table 1. Among these values, the basal ionic permeabilities (P_C and P_A) are within the experimental ranges for membrane permeability coefficients of Na^+ and Cl^- (e.g., see [36]). The extracellular ionic concentrations (C_e and A_e) could correspond to those of an external saline ambient (e.g., to culture conditions with concentrations of Na^+ and Cl^- similar to those of transcellular animal fluids [37]). The enzyme densities (N_T and M_T) fall within the range of the corresponding experimental values for some electrogenic enzymes [7,38,39]. The values chosen for K_1 and K_2 are arbitrary, although

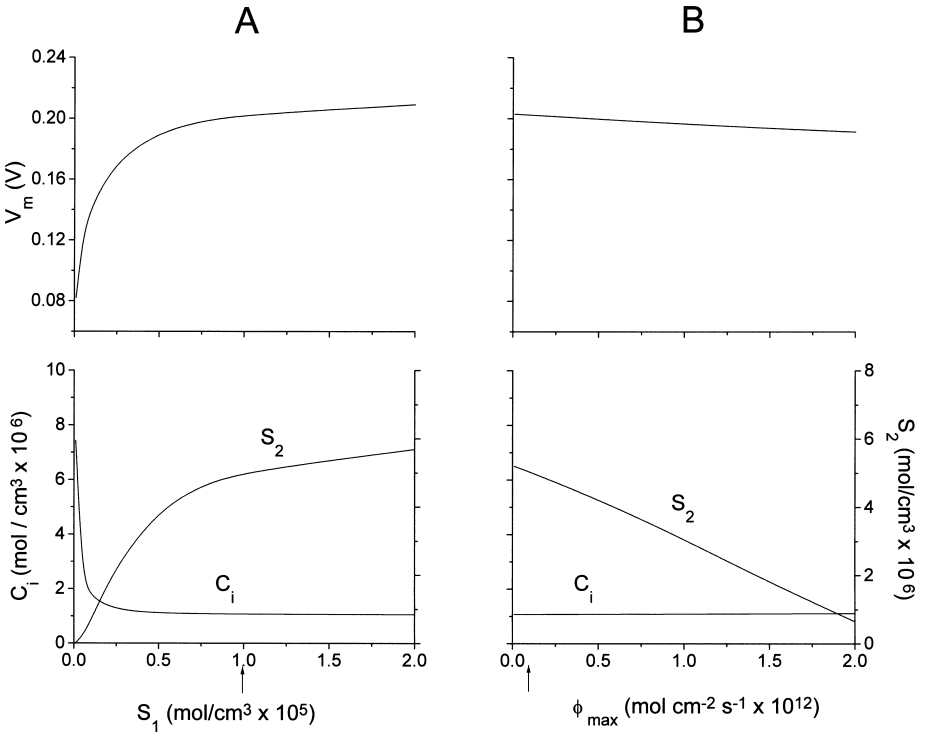

Fig. 3. Plots of the steady-state values of V_m, C_i and S_2 vs. S_1 (A) and vs ϕ_{max} (B). The rest of the parameter values as in Table 1. The arrow indicates the reference state MI (Eq. 4a).

of the order of magnitude of the equilibrium constants of several reactions that constitute energy sources for the active transport of Na^+ in microorganisms, like the hydrolysis of ATP [40], the decarboxylation of succinate to propionate [26], or the oxidation of NADH to NAD^+ [40]. Thus, for example, for the case of *Propionigenium modestum* [26], the pair (S_1/P_1) could represent the pair (succinyl CoA/propionyl CoA) while (S_2/P_2) would correspond to (ATP/ADP); for the case of *Klebsiella pneumoniae* [41] and *Haemophilus influenzae* [35] they would represent the pairs (NADH/NAD^+) and (ATP/ADP), respectively. A spherical microorganism with a radius of 1.4×10^{-4} cm (1.4 μm) would have a volume of 1.15×10^{-11} cm^3 and a total surface area of 2.46×10^{-7} cm^2. We assumed that the effective permeant area (A_c) is slightly smaller than this value (Table 1). The reference value for ϕ_{max} (Table 1) corresponds to a relatively high rate of metabolic expenditure. For the numerical values employed for the geometrical parameters A_c and V_c, ϕ_{max} would correspond to a turnover rate of 10^{-9} mol cm^{-3} s^{-1} (equal to (A_c/V_c) ϕ_{max}), a value in fair agreement with the basal turnover rate of ATP in mitochondria [42]. For the time-dependent effects of S_1, we employed a time constant (θ) of 50 s (Eq. 3).

The other parameters of the model were heuristically determined by a trial-and-error method, in order to obtain a plausible behavior of the model. Thus, the values for the rate constants of the enzymatic reactions were adjusted to obtain values for the kinetic parameters (e.g., maximum fluxes and

Table 1
Numerical values of the parameters

A_c: 10^{-7} cm^2	V_c: 10^{-11} cm^3
P_C: 6×10^{-9} cm s^{-1}	P_A: 10^{-7} cm s^{-1}
C_e: 1.4×10^{-4} mol cm^{-3}	A_e: 1.4×10^{-4} mol cm^{-3}
N_T: 4×10^{-12} mol cm^{-2}	M_T: 5×10^{-12} mol cm^{-2}
S_1: 10^{-5} mol cm^{-3}	P_1: 10^{-7} mol cm^{-3}
k_{01}: 10^6 mol^{-2} lt^2 s^{-1}	k_{10}: 1 s^{-1}[a]
$l_{01}°$: 10^3 mol^{-2} lt^2 s^{-1}	$l_{10}°$: 10^2 s^{-1}
p_{01}: 10^7 mol^{-2} lt^2 s^{-1}	p_{10}: 0.417 s^{-1}[a]
$q_{01}°$: 10^5 mol^{-2} lt^2 s^{-1}	$q_{10}°$: 10^3 s^{-1}
K_1: 10^5	K_2: 2.4×10^5
ϕ_{max}: 10^{-13} mol cm^{-2} s^{-1}	K_{S_2} : 5×10^{-8} *mol* cm^{-3}
T_2: 10^{-5} mol cm^{-3}	q: 10^{-6} mol cm^{-3}

[a]Determined from the detailed balance conditions (Eq. A4 and similar).

half-saturation constants, see Appendix) consistent with those experimentally determined for some electrogenic enzymes [38,39]. The half-saturation constant for the rate of metabolic consumption of S_2 (K_{S_2}) was arbitrarily chosen, the only restrictive criteria employed was to obtain a plausible steady-state dependence.

The reference states satisfy the steady-state for the parameter values listed in Table 1. We determined two reference states, MI and MII, corresponding to S_1 equal to 10^{-5} (Table 1) and 5×10^{-7} mol cm^{-3}, respectively (the rest of the parameter values as in Table 1):

MI : $V_m\ (0) = 0.2023$ V; $C_i\ (0) =$

1.07×10^{-6} mol cm^{-3}; $A_i\ (0) = 7\times10^{-8}$ mol cm^{-3};

$S_2\ (0) = 5.03\times10^{-6}$ mol cm^{-3};

$P_2\ (0) = 4.97\times10^{-6}$ mol cm^{-3}. (4a)

MII : $V_m(0) = 0.1218$ V; $C_i(0) =$

2.46×10^{-6} mol cm^{-3}; $A_i(0) = 1.46\times10^{-6}$ mol cm^{-3};

$S_2(0) = 0.21\times10^{-6}$ mol cm^{-3};

$P_2(0) = 9.79\times10^{-6}$ mol cm^{-3}. (4b)

MI and MII represent high and low energy states, respectively. Since there is no sufficient experimental evidence to justify their consideration as possible physiological states of particular microorganisms, the reference states given by Eqs. 4a and 4b are arbitrary, and only intended to be employed for the illustrative studies performed in this work. Although MII corresponds to a low energy condition, it is still far from the close-to-equilibrium situation characteristic of several fermentative bacteria employing decarboxylation reactions as primary energy sources [32]. In this latter cases, stoichiometric transport ratios larger than the 1C:1S_1 considered here might be necessary to accomplish the coupled synthesis of ATP [26].

3.3. Effect of the parameters on the steady-state

Fig. 3A,B shows the dependence of the steady-state with two parameters that reflect the metabolic condition of the microorganism: the internal concentration of the nutrient (S_1) and the maximum rate of metabolic consumption of the energetic metabolite S_2 (ϕ_{max}), respectively. For the interval considered, and as could have been expected, both energetic components of the electrochemical gradient of C significantly increase with S_1: V_m increases and C_i decreases (Fig. 3A). Correspondingly, S_2 increases. While V_m changes in a relatively smooth fashion, the curve for C_i is almost biphasic (see legend to Fig. 4A). The system exhibits saturation kinetics for V_m, in agreement with previously demonstrated properties of electrogenic enzymes [16]. Therefore, the system is not significantly capable of storing further energy by means of the energetic intermediate beyond a certain value of S_1 (for the case considered, approximately equal to 2×10^{-5} mol cm^{-3}). As could have been expected, S_2 decreases with ϕ_{max} (Fig. 3B). Since, for the parameter values considered, E_1 is the main electrogenic enzyme (that is, the main contributor to V_m, see legend to Fig. 4A,B), the modifications determined by ϕ_{max} on S_2 (and, correspondingly, on P_2) do not noticeably affect the membrane potential or the internal concentration of C. Fig. 3B therefore reveals that, in the interval explored, the system is capable of complying with a relatively large range of the metabolic requirement without significantly affecting its energetic capacity. In other words, the system can achieve physically meaningful steady-states (e.g., from a mathematical point of view, maintaining positive steady-state values of S_2) for relatively large values of ϕ_{max}. Within that interval, the changes provoked by ϕ_{max} on S_2 are purely kinetic, since they do not affect the components of the energetic intermediate (V_m and C_i).

Fig. 4 shows the dependence of the steady-state with the membrane densities of the electrogenic enzymes E_1 and E_2 (N_T and M_T, respectively). From the inspection of this figure it can be concluded that, for the parameter values considered, E_1 is the main electrogenic enzyme. This is basically a consequence of the particular choice of values for N_T and ϕ_{max} (Table 1). From Eqs. A8 and A11, in the steady-state $-J_2 \le \phi_{max}$, it can be demonstrated that, even for significantly large values of ϕ_{max} (cf. Fig. 3B), in the steady-state condition $J_1 \gg \phi_{max}$. Therefore, from the above relationship between J_2 and ϕ_{max},

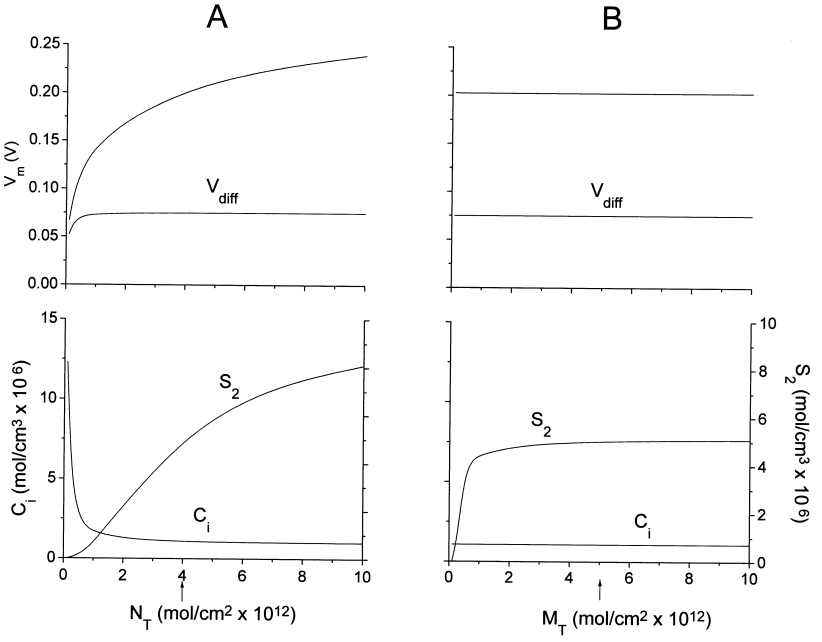

Fig. 4. Plots of the steady-state values of V_m, C_i and S_2 vs. the membrane density of E_1 (N_T) (A) and vs. the membrane density of E_2 (M_T) (B). The rest of the parameter values as in Table 1. The arrow indicates the reference state MI (Eq. 4a). V_{diff} is the diffusive membrane potential (Eq. A10).

the electroneutral condition (Eqs. 1b and A11) is approximately given by $-J_1+J_C=0$. As a consequence, the steady-state value of V_m is predominantly determined by E_1 and by the electrodiffusion of C. As mentioned above, this approximation remains valid for significantly large, possibly non-physiological, values of ϕ_{max} (Fig. 3B) and for relatively low values of N_T.

The predominance of E_1 is clearly revealed in Fig. 4A, where the membrane potential (V_m) is shown to increase significantly with N_T throughout the whole interval considered. We have previously demonstrated the existence of an approximately linear dependence between V_m and the enzyme density for a relatively large interval of density values of the dominant electrogenic enzyme [16]. At higher values of N_T, V_m converges to an asymptotic value [16] exclusively determined by terms provided by E_1 (not shown). In turn, C_i decreases with N_T, towards the asymptotic minimum value (equal to q) determined by the obligatory conservation condition given by Eq. 2. In this respect, it must be noticed that C is the only diffusible cation of the system studied here. Therefore, C is the only intracellular cation with variable concentration and, at minimum, it has to counterbalance an amount of excess negative charges pro-

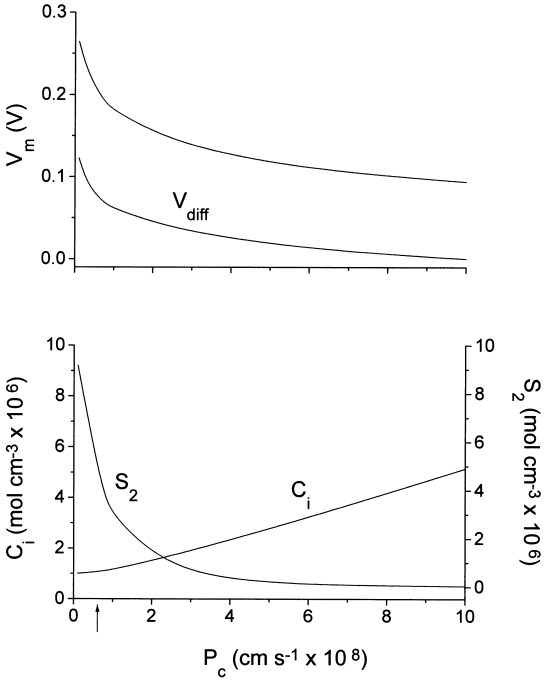

Fig. 5. Plots of the steady-state values of V_m, C_i and S_2 vs. the ionic permeability of C (P_C). The rest of the parameter values as in Table 1. The arrow indicates the reference state MI (Eq. 4a). V_{diff} is the diffusive membrane potential (Eq. A10).

vided by fixed intracellular anions (q). The electroneutral imposition implicit in the model (Eq. 1b) determines that, for values of C_i higher than q, non-zero internal concentrations of A will counterbalance the difference. C_i already acquires the asymptotic minimum value at relatively low values of N_T. Since P_C remains constant, the consequence is that the diffusive potential (V_{diff}, Eq. A10) also achieves an asymptotic value for those values of N_T. For the interval studied, S_2 increases with N_T. From the above, this is a direct consequence of the increase in V_m determined by increasing densities of E_1. For the parameter values considered here, E_2 does not affect any of the components of the energetic intermediate (Fig. 4B). However, it does affect S_2, which increases with M_T following saturation kinetics governed by ϕ_{max}, as a consequence of the consumption of the metabolite (see legend to Fig. 3B). From the above we may conclude that, for the parameter values considered here (Table 1), the amount of energy stored in the coupling intermediate mainly depends on the activity of E_1.

Fig. 5 shows the dependence of the steady-state with the ionic permeability of C (P_C). As can be seen, the increase in P_C determines dramatic changes in the system. The augmented ionic permeability determines an increase in C_i, which in turn produces a significant decrease both in the total V_m and in the electrodiffusive component (V_{diff}). In this respect, the increase in P_C produces analogous consequences to the decrease in N_T below certain critical values (see Fig. 4A). As can also be concluded from the analysis of Figs. 3A,B and 4A,B (see above), S_2 is extremely sensitive to changes in V_m, therefore its steady-state concentration decreases to a negligible minimum value in response to increases in P_C. In particular, Fig. 5 reveals that the system is extremely sensitive to changes in P_C in the neighborhood of its reference value (Table 1). Thus, decreases in P_C greatly increase the amount of energy stored via the coupling intermediate, fundamentally by means of the electrical component. Correspondingly, as a consequence of this increase in V_m, S_2 increases significantly with decreasing ionic permeability.

3.4. Dynamic effects of modifications in S_1 and ϕ_{max}

The effect of a significant decrease in S_1 (from

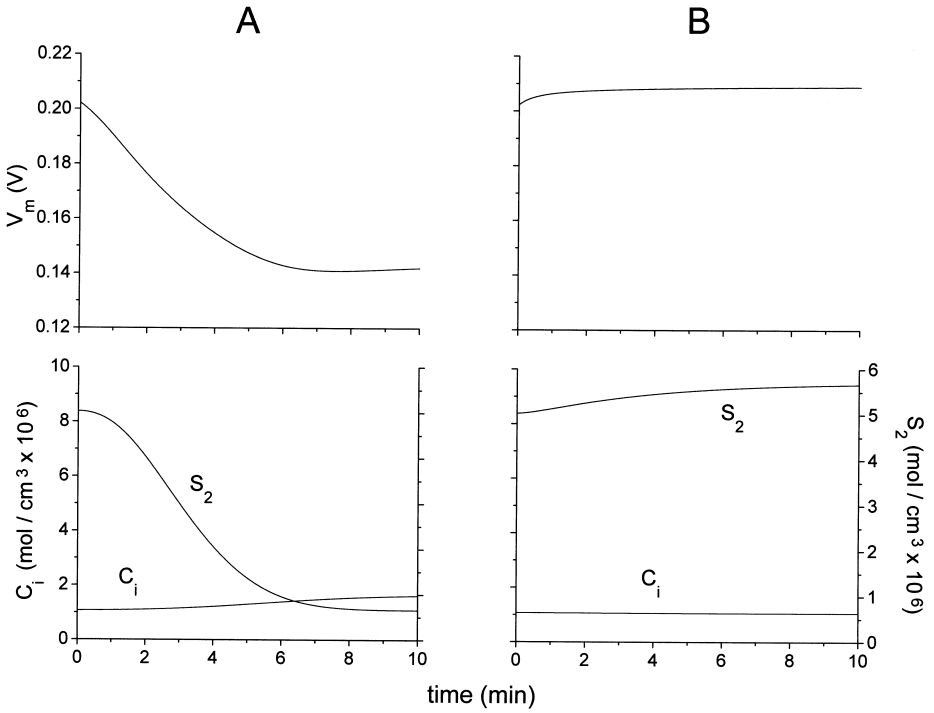

Fig. 6. Dynamic response of the model to a decrease in S_1 (from $S_1(0) = 10^{-5}$ to $S_1(\text{inf}) = 10^{-6}$ mol cm^{-3}, Eq. 3)(A) and to an increase in S_1 (from $S_1(0) = 10^{-5}$ to $S_1(\text{inf}) = 2 \times 10^{-5}$ mol cm^{-3}, Eq. 3) (B). V_m, C_i and S_2 are plotted as functions of time. Initial state for A and B: reference state MI (Eq. 4a). The rest of the parameter values as in Table 1.

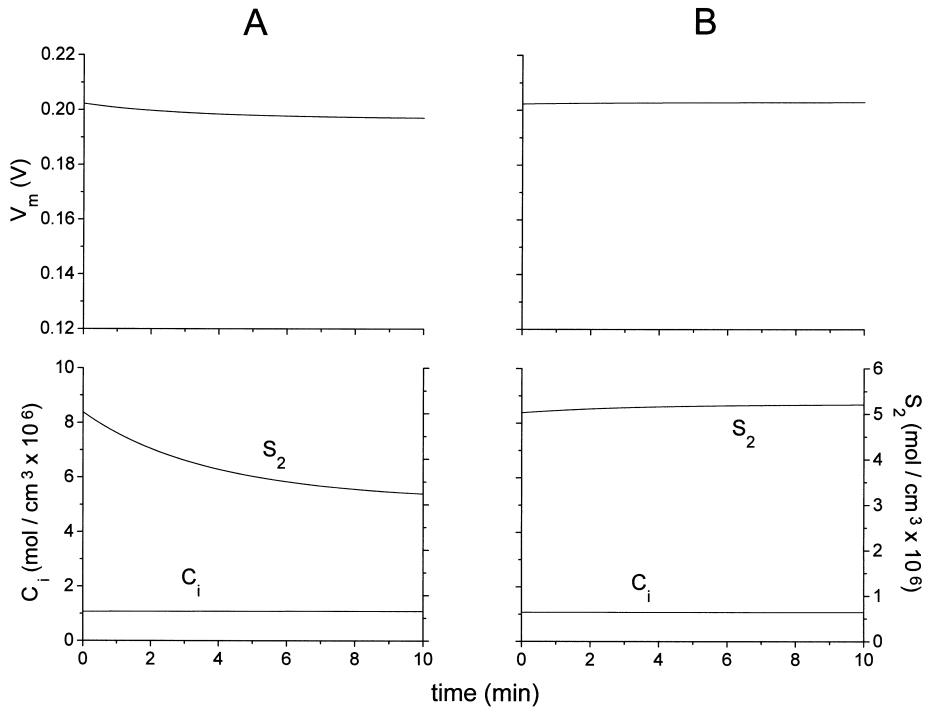

Fig. 7. Dynamic response of the model to an increase in ϕ_{max} (from its reference value (Table 1) to 10^{-12} mol cm^{-2} s^{-1}) (A) and to a decrease in ϕ_{max} (from its reference value (Table 1) to 10^{-14} mol cm^{-2} s^{-1}) (B). V_m, C_i and S_2 are plotted as functions of time. Initial state for A and B: reference state MI (Eq. 4a). The rest of the parameter values as in Table 1.

$S_1(0) = 10^{-5}$ to $S_1(\text{inf}) = 10^{-6}$ mol cm^{-3}, Eq. 3) on the time-dependent behavior of the model is shown in Fig. 6A, for the case of an initial condition given by the reference state MI (Eq. 4a). As can be seen, the main effect is a large decrease in V_m, which is a consequence of the fact that E_1 is the dominant electrogenic enzyme and main contributor to the membrane potential (see above). C_i increases only slightly, as a consequence of the fact that, in spite of the diminution in S_1, E_1 still maintains a larger relative contribution to V_m than the electrodiffusion of C (a predominance of P_C would determine a larger influx of C). Further decreases in S_1 would therefore produce more dramatic modifications, in particular, they would significantly increase C_i (cf. Fig. 3A). The decrease in V_m in turn determines a large decrease in S_2 (see legend to Fig. 3A,B and 4A,B). The inverse effect is obtained when S_1 is increased from its initial reference value ($S_1(0) = 10^{-5}$ mol cm^{-3}) to $S_1(\text{inf}) = 2 \times 10^{-5}$ mol cm^{-3} Eq. 3, Fig. 6B. In this 'S_1 pulse' experiment, the initial state of the system also corresponds to state MI (Eq. 4a). As can be seen, the increases provoked on V_m and S_2 are small, as a consequence of the fact that, for the initial value of S_1 considered, the system is already near saturation (cf. Fig. 3A).

The effect of a significant increase in ϕ_{max} (from its value in Table 1 to 10^{-12} mol cm^{-2} s^{-1}) on the time-dependent behavior of the model is shown in Fig. 7A, also for the case of the reference state MI (Eq. 4a). As could have been expected (cf. Fig. 3B), the only significant effect is a decrease in S_2, not associated to modifications in the energetic intermediate (e.g., in V_m or C_i, see legend to Fig. 3A,B). Conversely, the only dynamic effect produced on the reference state MI (Eq. 4a) by an important decrease in ϕ_{max} (from its reference value (Table 1) to 10^{-14} mol cm^{-2} s^{-1}, Fig. 7B) is a small increase in S_2. Similarly as the case of the modifications produced by S_1 (see Fig. 6A,B), the transient phases provoked by the perturbations of the system consist in monotonous relaxations to the new steady-states.

3.5. Dynamic behavior of particular cases of the model: constant V_m and constant C_i

Fig. 8A,B shows the effects of an increase in S_1 on the dynamic behavior of the model, for the cases

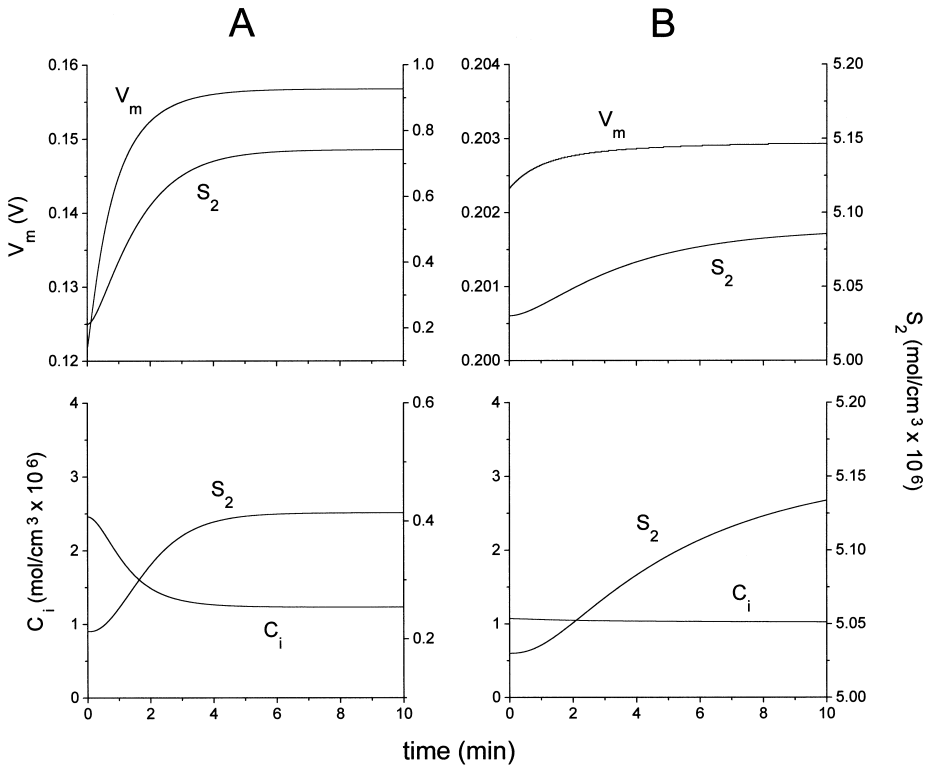

Fig. 8. Dynamic responses of the model to an S_1 pulse of 5×10^{-7} mol cm^{-3} [from $S_1(0)=5\times10^{-7}$ to $S_1(\text{inf})=10^{-6}$ mol cm^{-3} (Eq. 3, Fig. 8A), and from $S_1(0)=10^{-5}$ to $S_1(\text{inf})=1.05\times10^{-5}$ mol cm^{-3} (Eq. 3, Fig. 8A)]. V_m, C_i and S_2 are plotted as functions of time. Initial state for A: reference state MII (Eq. 4b). Initial state for B: reference state MI (Eq. 4a). Upper panels: the model was run maintaining C_i constant at its corresponding initial value. Lower panels: the model was run maintaining V_m constant at its corresponding initial value. The rest of the parameter values as in Table 1.

where: (a) C_i was maintained constant ('C_i-clamp' experiments, Fig. 8A,B, upper panels), and (b) V_m was maintained constant ('V_m-clamp' experiments, Fig. 8A,B, lower panels). For the simulations shown in Fig. 8A, the initial state of the system corresponded to the reference state MII whereas for those shown in Fig. 8B the initial state corresponded to the reference state MI (Eqs. 4b and 4a), respectively). For both cases the S_1 pulse was set equal to 5×10^{-7} mol cm^{-3}. Hence, for the simulations shown in Fig. 8A, S_1 changed from $S_1(0)=5\times10^{-7}$ to $S_1(\text{inf})=10^{-6}$ mol cm^{-3}; for those shown in Fig. 8B, from $S_1(0)=10^{-5}$ to $S_1(\text{inf})=1.05\times10^{-5}$ mol cm^{-3} (Eq. 3). For comparison, we calculated the free energy variations produced in the different cases as:

$$\Delta X_{elec} = F\,[(V_m)_{final}-(V_m)_{initial}];\ \Delta X_{conc} = R\,T\,[\ln\,(C_e/C_i)_{final}-\ln\,(C_e/C_i)_{initial}], \quad (5)$$

where ΔX_{elec} and ΔX_{conc} are the free energy changes in the electrical and concentration components, respectively, of the electrochemical gradient of C, and where F, R and T have their usual meanings. We assumed that $T=310$ Kelvin. In order to obtain the corresponding energy balances (Eq. 5), the final steady-state values of the variables were considered (not yet achieved in all the runs shown in Fig. 8)

For the cases where the initial state was MII (Fig. 8A), the effects produced by the S_1 pulse on the two models were notorious. For the C_i-clamp simulation (upper panel), the increase in S_1 determined an important increase in V_m and, consequently, an increase in S_2. For the V_m-clamp simulation (lower panel), the increase in S_1 determined an important decrease in C_i and, in turn, an increase in S_2. The extra amount of energy accumulated in each case in the form of the energetic intermediate, due to the S_1 pulse, was (Eq. 5):

For the C_i – *clamp simulation :*

$\Delta X_{elec} = F\,[(V_m)_{t=3600\,s} - (V_m)_{t=0}] =$

3373.9 Joule/mol.

For the V_m – *clamp simulation* :

$\Delta X_{conc} = RT\,[\ln (C_e/C_i)_{t=3600\,s} - \ln (C_e/C_i)_{t=0}] =$

1779.1 Joule/mol. (6a)

For the cases where the initial state corresponded to the reference state MI (Fig. 8B), the effects produced by the S_1 pulse on the two models were qualitatively similar to those shown in Fig. 8A, but negligible. Thus, V_m increased and C_i decreased in the C_i-clamp and V_m-clamp simulations, respectively, in insignificant amounts. This is reflected in the thermodynamic balance corresponding to each case:

For the C_i – *clamp simulation :*

$\Delta X_{elec} = F\,[(V_m)_{t=3600\,s} - (V_m)_{t=0}] = 59.4$ Joule/mol.

For the V_m – *clamp simulation* :

$\Delta X_{conc} = R\,T\,[\ln (C_e/C_i)_{t=3600\,s} - \ln (C_e/C_i)_{t=0}] =$

118.5 Joule/mol. (6b)

A comparison between Eqs. 6a and 6b suggests that, under the steady-state condition given by Eq. 4a (reference state MI), the system is close to the saturation of any of the components of the energetic intermediate (V_m or C_i). In this respect it is interesting to note that, in the complete model, S_1 already produces negligible effects on C_i in the neighborhood of its reference value corresponding to the microorganism state MI (cf. Fig. 3A). The state given by Eq. 4b is far from saturation, as is revealed by the fact that the S_1 pulse is capable of eliciting an important response of energy accumulation in both the C_i-clamp and V_m-clamp simulations (Eq. 6a). However, the C_i-clamp condition is capable of storing more energy (in the form of the electrical component) than the V_m-clamp condition (in the form of the concentration component), as revealed from the results shown in Eq. 6a.

The time constants of the two types of simulations are notoriously different. While, for the C_i-clamp simulations (Fig. 8A,B, upper panels), V_m exhibits a rapid tendency to achieve a new steady-state value, the change in C_i in the course of the V_m-clamp simulations (Fig. 8A,B, lower panels) takes place at a significantly slower pace. This property is particularly notorious for the case of the far-from-saturation state MII (Fig. 8A). It is an immediate consequence of the difference between the natural time scales of the changes in V_m and the changes in any ionic concentration [1,21]. This difference has been implicitly assumed in this study, by the employment of the stationary Eq. 1b as a solution for the time dependence of V_m (Appendix), instead of an explicit differential equation. The transient behaviors shown in Fig. 8 are also determined by the particular value employed for the time constant (θ) governing the modifications induced on the parameter S_1 (Eq. 3).

4. Conclusions

1. The model studied here exhibits the elementary kinetic and thermodynamic properties characteristic of a membrane system performing energy coupling via a chemiosmotic mechanism. Thus, the intermediate in the coupling process (the electrochemical gradient of C) is capable of storing energy provided by the nutrient (S_1) and of employing it for the synthesis of an energetic metabolite (S_2). Also, modifications in the ionic permeability (P_C) produce significant changes in both components of the energetic intermediate, a property consistent with the uncoupler role attributed to ionic leaks in energy storing membranes.
2. For the physiological range of values of the enzyme densities and of the rate of metabolic consumption of the energetic metabolite, the enzyme coupling the transport of the ionic ligand to the donor reaction (E_1) represents the relevant contributor to the membrane potential. Hence, the energy level achieved by the energetic intermediate and, correspondingly, the concentration of the energetic metabolite, are extremely sensitive to its enzymatic activity. As a consequence, the concentration of the energetic metabolite may change in response to changes in the metabolic usage (rep-

resented by modifications in ϕ_{max}) or in the activity of the electrogenic enzyme catalyzing its synthesis (E_2), without affecting the energy level of the coupling intermediate.

3. This study provides some arguments in favor of the notion that the electrical potential difference represents the relevant kinetic component of the energetic intermediate:
   - 3.1. The changes in the energetic metabolite mostly follow changes in the membrane potential. This is a consequence of the fact that the membrane potential is subject to less restrictive conditions than the intracellular concentration of the diffusive cation. The diffusive cation cannot decrease below a minimum value, as a consequence of the electroneutral imposition. In this respect, it must be noticed that this work already assumed a relatively large extracellular concentration of the diffusible cation and imposed a very low minimum value for its intracellular concentration.
   - 3.2. For analogous inputs in nutrient (equal S_1 pulses), the membrane potential represents a faster source of free energy storing than the concentration component. Also, for far-from-saturation conditions, the membrane potential is capable of storing a larger amount of energy. This is also a consequence of the restrictions imposed on the intracellular concentration of the diffusive cation by the electroneutral condition, which precludes further modifications in the concentration component (see previous paragraph).
4. Finally, the model studied here could represent the simplest situation. Further studies extending this basic model for the case of more realistic situations would require to explore, among others, the effects of:
   - 4.1. The introduction of non-Ohmic terms in ionic electrodiffusion.
   - 4.2. The introduction of slippage in the enzyme models.
   - 4.3. The introduction of molecular stoichiometric ratios different than one in the transport processes mediated by the electrogenic enzymes. This might produce a model capable of functioning under lower energy conditions than the ones considered here (e.g., to sustain a similar or even larger thermodynamic force for the reaction $S_2 \leftrightarrow P_2$ from a lower one provided by the reaction $S_1 \leftrightarrow P_1$).
   - 4.4. The application of the model to the case of protons. The analysis of explicit kinetic models of the processes of energy coupling where the intermediate is the electrochemical gradient of protons may provide further elements to comprehend why this cation was selected in the course of the evolution of this type of processes.

In summary, the model studied here represents a plausible description of the elementary kinetic aspects of energy coupling in supramolecular membrane systems. Its fundamental properties might be characteristic of some microorganisms employing the electrochemical gradient of Na^+ as intermediate for the coupling process. Its main contribution consists in proposing a plausible modeling procedure and methodological approach to describe dynamic and stationary properties of elementary processes of energy coupling in membranes.

Acknowledgements

This work was supported by grants from the Programa para el Desarrollo de las Ciencias Básicas (PEDECIBA) and from the Comisión Sectorial de Investigación Científica (CSIC) de la Universidad de la República, Uruguay.

Appendix

1. Glossary of symbols

1. Variables:
   - C_i, A_i: intracellular concentrations of C and A
   - S_2, P_2: concentrations of S_2 and P_2
   - V_m: electrical potential difference across the plasma membrane
   - t: time

2. Parameters:

A_c: effective permeant area of the microorganism surface
V_c: volume of the microorganism
P_C, P_A: ionic permeability coefficients of C and A
C_e, A_e: extracellular concentrations of C and A
N_T, M_T: total density of enzymes E_1 and E_2, respectively
S_1, P_1: concentrations of S_1 and P_1
k_{01}, k_{10}, l_{01}, l_{10}: rate constants governing the transitions of E_1
p_{01}, p_{10}, q_{01}, q_{10}: rate constants governing the transitions of E_2
K_1: equilibrium (dissociation) constant of the reaction $S_1 \leftrightarrow P_1$
K_2: equilibrium (dissociation) constant of the reaction $S_2 \leftrightarrow P_2$
ϕ_{max}, K_{S_2}: maximum flux and half-saturation constant of the metabolic consumption of S_2
T_2: sum of S_2 and P_2
q: difference between C_i and A_i

2. Transport of C mediated by the electrogenic enzymes

The active transport of C mediated by E_1 is described by the two-state diagram shown in Fig. 2. In this diagram, N_0 and N_1 are the intermediate states of the electrogenic enzyme, and k_{01}, k_{10}, l_{01} and l_{10} are the (true) rate constants governing the corresponding transitions. The meaning of the rest of the symbols is specified in the glossary (see Section 1). The steady-state analysis of this type of diagram has already been performed [25], we show here the main expressions. In the steady-state, the cycle flux J_1 (considered positive in the clockwise direction) can be expressed, employing the diagram method [43], as:

$$J_1 = (N_T/\Sigma_1)\,(k_{01}\,l_{10}\,S_1\,C_i - k_{10}\,l_{01}\,P_1\,C_e), \qquad \text{(A1)}$$

where N_T is the total amount of the enzyme and where Σ_1 is the sum of all the directional diagrams of the model, given by:

$$\Sigma_1 = k_{01}\,S_1\,C_i + l_{01}\,P_1\,C_e + k_{10} + l_{10}.$$

For the case that $P_1 = 0$ and $C_i = C_e = C$, we obtain from Eq. A1 the maximum flux (J_{m,S_1}) and Michaelis constant (K_{m,S_1}) for S_1:

$$J_{m,S_1} = N_T\,l_{10} \textit{ and } K_{m,S_1} = (k_{10} + l_{10})/k_{01}\,C. \qquad \text{(A2a)}$$

Analogously, for P_1:

$$J_{m,P_1} = N_T\,k_{10} \textit{ and } K_{m,P_1} = (k_{10} + l_{10})/l_{01}\,C. \qquad \text{(A2b)}$$

The rate constants l_{01} and l_{10} are assumed to depend on V_m according to:

$$l_{01} = l_{01}^{\circ}\,exp\,[FV_m/(2RT)];\; l_{10} = l_{10}^{\circ}\,exp\,[-FV_m/(2RT)], \qquad \text{(A3)}$$

where l_{01}° and l_{10}° are independent of V_m, and where F is Faraday's constant, R the gas constant and T the absolute temperature (310 Kelvin).

The detailed balance condition imposes the following restriction on the rate constants:

$$K_1 = k_{01}\,l_{10}^{\circ}/(k_{10}\,l_{01}^{\circ}), \qquad \text{(A4)}$$

where K_1 is the equilibrium (dissociation) constant of the reaction $S_1 \leftrightarrow P_1$.

Since there is only one cycle, the active flux of C mediated by E_1 (considered positive in the outward direction) is equal to J_1 (Eq. A1).

The diagram describing the active flux of C mediated by E_2 is formally similar to the one corresponding to E_1 (Fig. 2). Hence, analogous expressions to the ones derived for E_1 can be obtained for the case of E_2. In particular, the active flux of C mediated by E_2 equals J_2:

$$J_2 = (M_T/\Sigma_2)\,(p_{01}\,q_{10}\,S_2\,C_i - p_{10}\,q_{01}\,P_2\,C_e). \qquad \text{(A5)}$$

In Eq. A5, M_T is the total amount of the enzyme and Σ_2 is the sum of all the directional diagrams of the model. Similarly as the case of E_1, we assume that the rate constants q_{01} and q_{10} depend on V_m according to:

$$q_{01} = q_{01}^{\circ}\,exp\,[FV_m/(2RT)];\; q_{10} = q_{10}^{\circ}\,exp\,[-FV_m/(2RT)], \qquad \text{(A6)}$$

where q_{01}° and q_{10}° are independent of V_m.

3. Electrodiffusion equations

We assumed that the basal electrodiffusive fluxes of C and A are given by the Goldman equation [10], as modified by Hodgkin and Katz [11], which we express as:

$$J_C = P_C\ \varepsilon_m\ [C_e\ exp\ (u/2) - C_i\ exp\ (-u/2)]$$
$$J_A = P_A\ \varepsilon_m\ [A_e\ exp\ (-u/2) - A_i\ exp\ (u/2)] \quad (A7)$$

with $u = F\ V_m/(RT)$ and $\varepsilon_m = u/[\exp\ (u/2) - \exp\ (-u/2)]$, and where P_C and P_A are the ionic permeability coefficients of C and A, respectively. F, R and T have their usual meanings (see Eq. A3).

4. Metabolic conversion of S_2

We also assumed that, under standard physiological conditions, the metabolic consumption of S_2 follows Michaelis kinetics:

$$\phi = \phi_{max}\ S_2/(K_{S2} + S_2), \quad (A8)$$

where ϕ_{max} is the maximum metabolic flux and K_{S_2} is the apparent half-saturation constant.

5. Stationary solution for V_m

For the particular values computed in each integration step for C_i and S_2, V_m was obtained as the root of Eq. 1b:

$$V_m = V_m\ (-J_1 - J_2 + J_C - J_A = 0) \quad (A9)$$

In Eq. A9, Eqs. A1, A5 and A7 were employed to express the ionic fluxes J_1, J_2, J_C and J_A. Similarly as in our previous studies [16,21], V_m was determined from Eq. A9 by an iterative procedure which yielded convergent solutions for all the simulations. In the absence of electrogenic transport (e.g., for $N_T = M_T = 0$), Eq. A9 permits to obtain the classical Goldman–Hodgkin–Katz [10,11] explicit equation for the diffusion potential [16], which for the case under consideration is given by:

$$(V_m)_{diff} =$$
$$(RT/F)\ \ln\ [P_C\ C_i + P_A\ A_e]/[P_C\ C_e + P_A\ (C_i - q)] \quad (A10)$$

6. Determination of the steady-state values

In the steady-state, Eq. 1a satisfies $dC_i/dt = dA_i/dt = dS_2/dt = -dP_2/dt = 0$, or

$$-J_1 - J_2 + J_C = J_A = -J_2 - \phi = 0. \quad (A11)$$

Similarly as the stationary calculation of V_m in the time-dependent studies (see above), the roots of Eq. A11 were determined by an iterative procedure [21], which yielded convergent solutions for the steady-state values of C_i, S_2, and V_m in all of the determinations.

References

[1] E. Jakobsson, Am. J. Physiol. 238 (1980) C196–C206.
[2] S.G. Schultz, Basic Principles of Membrane Transport, Cambridge University Press, Cambridge, 1980.
[3] J.H. Byrne, S.G. Schultz, An Introduction to Membrane Transport and Bioelectricity, Raven Press, New York, 1988, pp. 66–92.
[4] S.R. Caplan, A. Essig, Bioenergetics and Linear Nonequilibrium Thermodynamics. The Steady-State, Harvard University Press, Cambridge, MA, 1983, pp. 348–388.
[5] H.V. Westerhoff, K. van Dam, Thermodynamics and Control of Biological Free-Energy Transduction, Elsevier, Amsterdam, 1987.
[6] P. Joliot, A. Verméglio, A. Joliot, Biochim. Biophys. Acta 1141 (1993) 151–174.
[7] P. Läuger, Electrogenic Ion Pumps, Sinauer, Sunderland, MA, 1991, pp. 3–14.
[8] J. Nedergaard, B. Cannon, in: L. Ernster (Ed.), Molecular Mechanisms in Bioenergetics, Elsevier, Amsterdam, 1992, pp. 385–420.
[9] M.D. Brand, L.-F. Chien, E.K. Ainscow, D.F.S. Rolfe, R.K. Porter, Biochim. Biophys. Acta 1187 (1994) 132–139.
[10] D.E. Goldman, J. Gen. Physiol. 27 (1943) 37–60.
[11] A.L. Hodgkin, B. Katz, J. Physiol. Lond. 108 (1949) 37–77.
[12] N.J. Mullins, K. Noda, J. Gen. Physiol. 47 (1963) 117–132.
[13] R.B. Moreton, J. Exp. Biol. 51 (1969) 181–201.
[14] J.A. Jacquez, Math. Biosci. 12 (1971) 185–196.
[15] R.A. Sjodin, in: M.P. Blaustein, M. Lieberman, (Eds.), Electrogenic Transport. Fundamental Principles and Physiological Implications, Raven Press, New York, 1984, pp. 105–127.
[16] J.A. Hernández, J. Fischbarg, L.S. Liebovitch, J. Theor. Biol. 137 (1989) 113–125.
[17] G.W.F.H. Borst-Pauwels, Biochim. Biophys. Acta 1145 (1993) 15–24.
[18] D.R. Scriven, Biophys. J. 35 (1981) 715–730.
[19] D.R. Lemieux, F.A. Roberge, P. Savard, J. Theor. Biol. 142 (1990) 1–33.

[20] J. Strieter, J.L. Stephenson, L.G. Palmer, A.M. Weinstein, J. Gen. Physiol. 96 (1990) 319–344.
[21] J.A. Hernández, E. Cristina, Am. J. Physiol. 275 (1998) C1067–C1080.
[22] H.V. Westerhoff, K. van Dam, in: L. Ernster (Ed.), Molecular Mechanisms in Bioenergetics, Elsevier, Amsterdam, 1992, pp. 1–35.
[23] H.-G. Holzhütter, W. Henke, W. Dubiel, G. Gerber, Biochim. Biophys. Acta 810 (1985) 252–268.
[24] B. Korzeniewski, W. Froncisz, Biochim. Biophys. Acta 1060 (1991) 210–223.
[25] U.-P. Hansen, D. Gradmann, D. Sanders, C.L. Slayman, J. Membr. Biol. 63 (1981) 165–190.
[26] P. Dimroth, Biochim. Biophys. Acta 1101 (1992) 236–239.
[27] P. Dimroth, Biochim. Biophys. Acta 1318 (1997) 11–51.
[28] P.H. Yancey, M.E. Clark, S.C. Hand, R.D. Bowlus, G.N. Somero, Sci. Wash. 217 (1982) 1214–1222.
[29] K.R. Hallows, P.A. Knauf, in: K. Strange, (Ed.), Cellular and Molecular Physiology of Cell Volume Regulation, CRC Press, Boca Raton, FL, 1994, pp. 3–29.
[30] H. Moo Kwon, J.S. Handler, Curr. Opin. Cell Biol. 7 (1995) 465–471.
[31] M. Dybas, J. Konisky, J. Bacteriol. 174 (1992) 5575–5583.
[32] P. Dimroth, B. Schink, Arch. Microbiol. 170 (1998) 69–77.
[33] K.D. Garlid, A.D. Beavis, S.K. Ratkje, Biochim. Biophys. Acta 976 (1989) 109–120.
[34] V.P. Skulachev, in: L. Ernster, (Ed.), Molecular Mechanisms in Bioenergetics, Elsevier, Amsterdam, 1992, pp. 37–73.
[35] M. Hayashi, Y. Nakayama, T. Unemoto, FEBS Lett. 381 (1996) 174–176.
[36] N. Sperelakis, in: N. Sperelakis (Ed.), Cell Physiology. Source Book, Academic Press, New York, 1995, pp. 61–66.
[37] F. Lang, in: R. Greger, U. Windhorst (Eds.), Comprehensive Human Physiology, Springer-Verlag, Berlin, 1996, pp. 1545–1556.
[38] D. Gradmann, J. Tittor, V. Goldfarb, Phil. Trans. R. Soc. Lond. B 299 (1982) 447–457.
[39] C.L. Slayman, D. Sanders, in: M.P. Blaustein, M. Lieberman (Eds.), Electrogenic Transport. Fundamental Principles and Physiological Implications, Raven Press, New York, 1984, pp. 307–322.
[40] A.L. Lehninger, D.L. Nelson, M.M. Cox, Principles of Biochemistry, 2nd edn., Worth Publishers, New York, 1993, pp. 375–377.
[41] P. Dimroth, A. Thomer, Arch. Microbiol. 151 (1989) 439–444.
[42] J.G. Reich, E.E. Sel'kov, Energy Metabolism of the Cell, Academic Press, New York, 1981, pp. 115–122.
[43] T.L. Hill, Free Energy Transduction in Biology, Academic Press, New York, 1977, pp. 1–32.